Neuromagnetic Instrumentation[1]

Fig. 1. A dual seven channel SQUID magnetometer used for magnetoencephalography. Courtesy of Biomagnetic Technologies, Inc. San Diego, CA, USA.

1. Introduction

The signal strengths associated with neural activity (fig. 2) require the use of extremely sensitive detection systems **(1)**. To date, the only instrument with the required sensitivity and bandwidth is the SQUID magnetometer **(2-6)**. This chapter will attempt to give an overview of current instrumental techniques used in neuromagnetic measurements. It is not intended to go into great detail of every aspect of SQUID instrumentation. For additional information, the reader is encouraged to refer to the more detailed articles referenced.

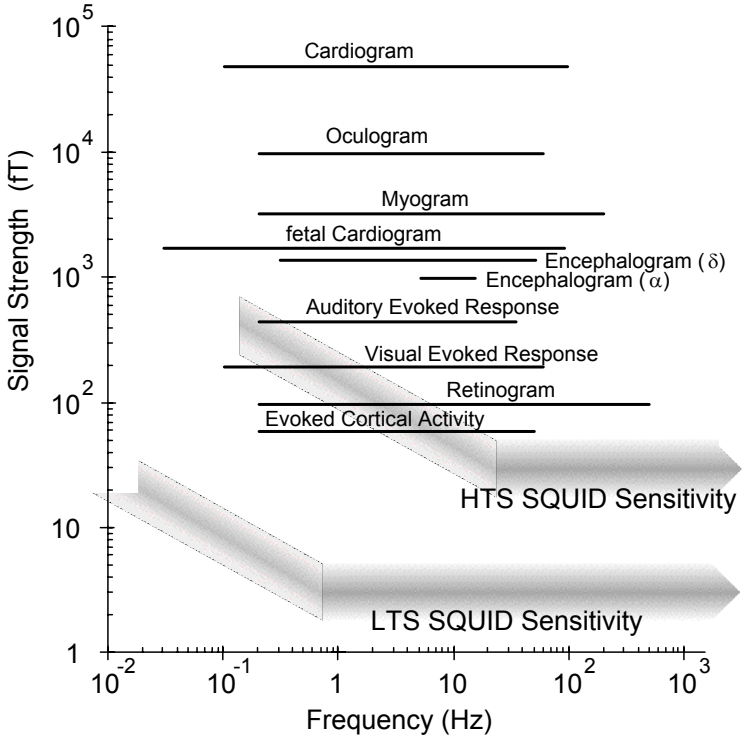

Fig. 2. Typical signal strengths and frequency ranges for various biomagnetic signals. 1 fT = 10^{-15} tesla

The components of a SQUID magnetometer used for neuromagnetic measurements typically consist of: a detection coil, which senses changes in the external magnetic field and transforms it into an electrical current; an input coil which transforms the resulting current into a magnetic flux, the SQUID sensor; and associated electronics which transform the applied flux into a room temperature voltage output. Both the SQUID

[1] Slightly revised June 2003

amplifier and the detection coils are superconducting devices. Thus some type of refrigerant (liquid helium) or refrigeration device is needed to maintain the SQUID (and detection coil) in the superconducting state. Additional signal conditioning electronics may be needed to improve signal-to-noise.

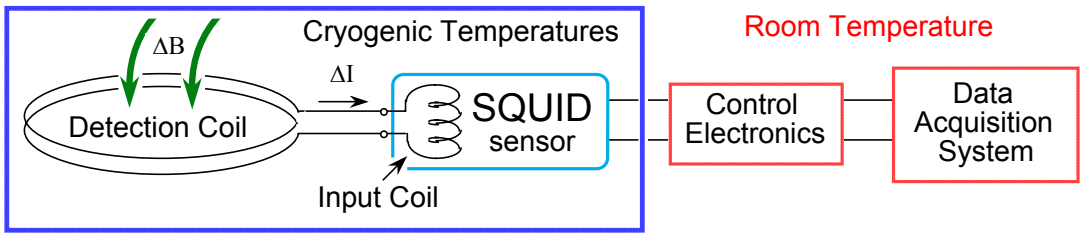

Fig. 3. Block diagram of SQUID magnetometer

2. The SQUID sensor

The term SQUID is an acronym for a SUperconducting QUantum Interference Device that utilizes the Josephson effect phenomena to measure extremely small variations in magnetic flux. The theory and operation of different types of SQUIDs is described in detail in the literature **(2,7,8)**. For a loop of superconducting wire interrupted by a normal, resistive, region, one would expect it to behave the same as a continuous loop of normal metal. I.e., a current flowing in the loop would quickly decay. In 1962, Brian Josephson **(9)** predicted the possibility of electrons tunneling from one superconducting region to another that had been separated by a resistive (insulating) barrier (usually called a "weak link"). For currents less than a critical current I_c that is characteristic of the weak link, a current can penetrate the resistive barrier with no voltage drop. Additionally, magnetic flux penetrating a superconducting loop must be quantized in units of a flux quantum $\phi_o = hc/2e$ (2.068×10^{-15} Webers). In conjunction with flux quantization, the Josephson effect can be used to measure changes in magnetic flux.

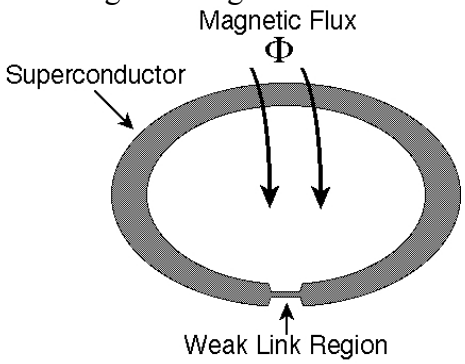

Fig. 4. SQUID loop with externally applied flux threading through the loop

Physically, the sensing element of a SQUID consists of a superconducting ring which is interrupted by one or more regions (Josephson junctions) that are either resistive or have such a low critical current that they become resistive far sooner than the rest of the ring or loop as it is sometimes referred to (fig. 4). Because of its superconducting nature, a SQUID must be operated below its transition temperature (T_c). The thermal energy required to destroy superconductivity rapidly goes to zero close to T_c **(8)**. Thus, for low noise operation, the SQUID should operate at a temperature below ½ T_c. For SQUIDs fabricated from materials such as niobium (T_c = 9.3 K), this corresponds to an operating temperature below 4.7 K. Operation at temperatures up to $^2/_3$ T_c are possible, but with a significant increase in noise.

The SQUID loop is connected to circuitry for detecting changes in the flux penetrating the loop. SQUIDs are operated as either rf or dc SQUIDs. The dc SQUID differs from the rf SQUID in the manner of biasing the Josephson junction and the number of junctions. The prefix rf or dc refers to whether the Josephson junction(s) is biased with an radiofrequency alternating current (rf) or direct (dc) current. In former case, flux changes are detected by a resonant tank circuit that is inductively coupled to the SQUID loop (the rf SQUID).

In the latter, the SQUID loop contains two Josephson junctions and a dc current is applied (the dc SQUID). Flux changes are detected by monitoring the voltage across the junctions. The noise mechanisms of the rf and dc SQUIDs are inherently different, with the dc SQUID offering more than two orders of magnitude advantage. With modern thin film fabrication techniques and improvements in control electronics design, the dc SQUID offers clear advantages over the rf SQUID for neuromagnetic applications. The demand for improved signal-to-noise requires the use of dc SQUIDs.

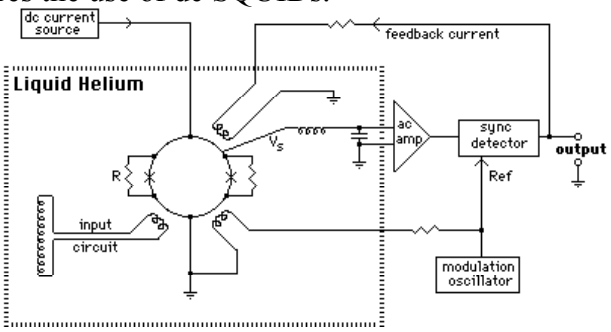

Fig. 5. Block diagram of a typical dc SQUID

dc SQUIDs (fig. 5) require two junctions whose characteristics are matched within a few percent. For thin film devices, this required the development of photolithography techniques. Flux is inductively coupled into the SQUID loop via an input coil which connects the SQUID to the experiment. The dc SQUID is biased with a dc current approximately equal to twice I_c and develops a dc voltage across the junctions. This voltage is a periodic function of the applied flux applied to the SQUID loop by the input coil. This output voltage can be amplified and used to generate a feedback current. This current is inductively coupled back into the SQUID loop to null the applied signal flux. As a result, the SQUID is "locked-up" at a single flux bias point, and the feedback current is a direct measure of changes in flux applied to the SQUID.
Because of the varying input impedances of SQUID sensors, the sensitivity of SQUID devices is best discussed in terms of the energy sensitivity:

$$E_N = L_{input} I_N^2 = \frac{\Phi_N^2}{L_{input}} \tag{1}$$

where L_{input} is the input inductance of the device, I_N is the current noise and Φ_N is the flux sensitivity. E_N has the units of Joules/Hertz and is often expressed in terms of Planck's constant $h = 6.6 \times 10^{-34}$ J/Hz. The minimum noise energy for a dc SQUID is given by **(10)**

$$E_N = 12\, k_B T \sqrt{L\, C} \tag{2}$$

where k_B is Boltzmann's constant, L is the inductance of the SQUID loop and C the capacitance of the junction. Substituting appropriate numbers indicates that the minimum noise energy (E_N) for a dc SQUID is on the order of h/2. Devices with sensitivities of ~ h have been constructed **(11)**. These extremely low noise levels are achieved by limiting dynamic range and avoiding feedback. The need for practical (useful) devices requires that feedback be used and that the SQUID have a reasonable dynamic range. Commercially available rf SQUIDs have noise levels of 10^{-28} J/Hz; commercial dc SQUIDs are typically ~ 10^{-30} J/Hz. Several laboratories have produced dc SQUIDs with noise levels below 10^{-31} J/Hz.

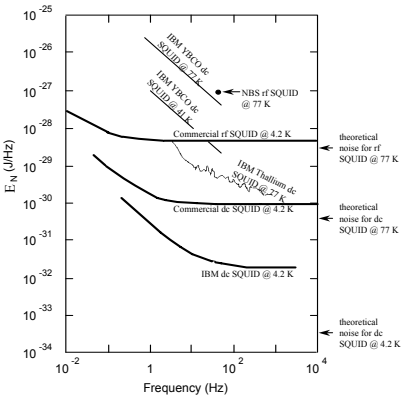

Fig. 6. Noise levels of various SQUID sensors. YBCO and Thallium refer to SQUID sensors made of high temperature superconducting materials **(ref. 27)** *please note this data is very old*. Equivalent HTS sensitivities are near the 10^{-30} level

In addition to the frequency independent (white) component of system noise, there exists a low frequency contribution that departs from flat frequency response as the frequency decreases (fig. 6). The relative amount of this "1/*f*"noise can be dependent on the ambient magnetic field when the SQUID sensor is cooled. When cooled in the earth's magnetic field, the point at which the 1/*f* noise equals the white (frequency independent) noise is typically ~ 1 Hz. Cooling the SQUID sensor in low ambient magnetic fields (less than 1 microtesla) may improve the 1/*f* performance by as much as an order of magnitude. A large contribution to this noise in some dc SQUIDs can arise from the presence of the dc current bias. By chopping the dc bias in combination with the conventional flux modulation techniques, it is possible to reduce this added 1/*f* noise. This double modulation approach **(12)** separates the original signal waveform from the noise associated with the dc bias, and can reduce 1/*f* noise at very low frequencies.

2.1. Sensor Configurations

Although it is possible to directly couple magnetic flux into the SQUID loop, environmental noise considerations (see fig. 14) make this difficult, if not impossible in an unshielded environment. In addition, the area of a typical SQUID loop is small (<10 mm^2) and its resulting sensitivity to external flux changes ($\Delta\Phi = A\ \Delta B$) small. Although a larger loop diameter would increase the SQUIDs sensitivity to external flux, it would also make it much more susceptible to environmental noise. For this reason, external flux is normally inductively coupled to the SQUID loop by a flux transformer. SQUIDs can also be fabricated as a planar device. In this configuration, the superconducting loop, Josephson junctions and coils (input, feedback and modulation) are patterned on the same device. Multilayer deposition techniques are used and coils are normally in the form of a square washer. The planar configuration leads to quite small devices, occupying only a few mm^3 compared to 5+ cm^3 (1.2 cm diameter x 5 cm) for a toroidal SQUID. This can be a significant advantage for multi-channel systems. Another advantage of the planar device is that it is possible to have the detection coils as part of the SQUID sensor, eliminating the need for separate (three-dimensional) detection coils. Such an integrated sensor has the potential to significantly reduce the complexity of constructing SQUID systems containing 100 or more channels.

2.2. Control Electronics

The system output voltage is the voltage drop across the feedback resistor in a negative feedback loop controlled by the SQUID electronics. The feedback signal is generated in response to changes in the output signal of the SQUID sensor. The output of the SQUID sensor is periodic in the field at the pickup coil. A Negative feedback (similar to a phase-locked loop technique) is used to maintain the system operating point at a particular (and arbitrary) flux quantum. When operated in this mode, the system is in a flux-locked loop. It should be noted that although total flux within the SQUID loop is in multiples of ϕ_o, by measuring the voltage drop across the feedback resistor, resolutions of external flux changes at the 10^{-5} ϕ_o level can be achieved. The linearity of flux-locked loop SQUID systems are typically better than 1 ppm.

If the input to the SQUID changes at a rate greater than the feedback circuit can follow, the output will exhibit occasional discontinuities or flux jumps. These jumps can result in an offset in the dc level. The maximum speed with which the output can follow the input is called the slew rate limit of the system. This can be given in terms of flux quanta/sec (referred to the SQUID loop) or as a change in current (amperes/sec referred to the input current). This places an upper limit on the bandwidth of the system. The typical bandwidth of commercially available SQUID systems is dc to 20+ kHz, much greater than any frequency of interest for neurological applications (fig. 2). A typical slew rate for SQUID electronics is 10^5 ~10^6 ϕ_o/sec (+ 10 ~ 100 mA/sec generated at a typical input coil).

It is important to realize that even though one may not need or want to observe rapidly changing signals, situations may arise when ambient noise (60 Hz for example) may determine the slew rate requirements of the system. To recover a signal from such interference, it is necessary that the system be able to track all signals present at the input, including the noise. When system response is sped up to handle very fast signals, sensitivity to radiofrequency interference (rfi) and spurious transients is also increased. Since ability to remain locked while subjected to strong electrical transients is greatest when the maximum slew rate is limited (slow), while ability to track rapidly varying signals is greatest when the maximum slew rate is greatest (fast), it is desirable to be able to match the maximum slew-rate capability to the measuring situation. As a matter of convenience, many commercial SQUID systems offer user selectable slew rates along with high-pass and low-pass filters for noise reduction. Additional features can include adjustable dc offsets and notch or comb filters.

2.3. SQUID Performance

Whether a rf or dc SQUID, we can consider the SQUID sensor as a black box that acts like a current to voltage amplifier with extremely high gain. In addition, it offers extremely low noise, high dynamic range, excellent linearity and a wide bandwidth that can extend down to dc. A typical SQUID sensor can provide a transfer function in excess of 10^7 volts/ampere. The input sensitivity can be better than 10^{-12} amperes/$\sqrt{Hz}$, equivalent to an energy sensitivity of 10^{-30} joules/hertz. Linearities can exceed 1 part in 10^7, dynamic ranges can exceed 165 dB and bandwidths typically extend from dc to hundreds of kHz. The input impedance of a SQUID in purely inductive and is typically 0.5 ~ 2 μH. These factors allow us to use the SQUID to design a system for the detection of magnetic fields orders of magnitude more sensitive than any other known device.

3. Input Circuits

Conceptually, the easiest input circuit to consider for detecting changes in magnetic fields that of a SQUID sensor connected to a simple superconducting pickup coil (fig. 7).

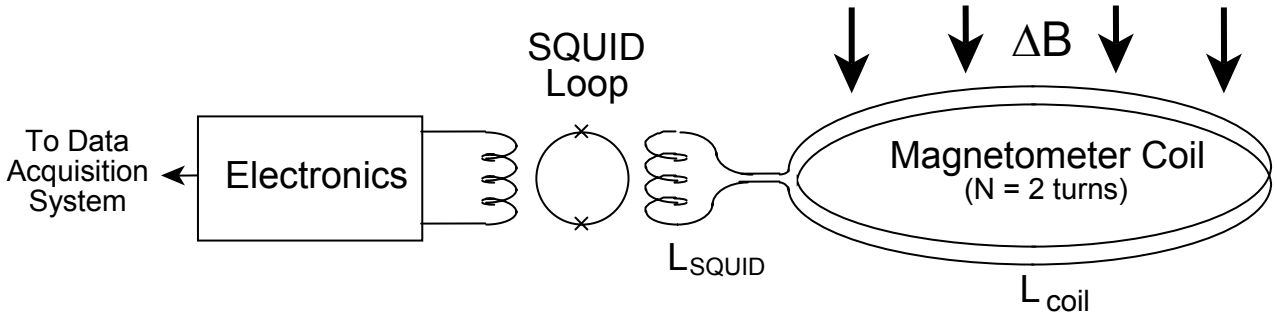

Fig. 7. Schematic diagram of typical SQUID input circuit

Since the total flux in a superconducting loop is conserved, any change in external field through the pickup coil will induce a current in the flux transformer which must satisfy

$$\Delta\Phi = NA\Delta B = (L_{coil} + L_{SQUID})\Delta I \qquad (3)$$

where ΔB is the change in applied field; N, A, and L_{coil} are the number of turns, area, and inductance of the pickup coil; L_{SQUID} is the input inductance of the SQUID; and ΔI is the change in current in the

superconducting circuit. We have ignored the inductance of the leads since it is usually negligible; a tightly twisted pair of 0.005" wires has a typical inductance of 0.3 μH/meter. If the lead inductance (L_{lead}) is not negligible, it must be added to L_{coil} and L_{SQUID}.

To calculate the sensitivity and noise level of a simple detection coil system, the inductance of the detection coil must be known. The inductance (in microhenries) of a flat, tightly wound, circular multi-turn loop of superconducting wire is given by **(13)**

$$\Delta B = 0.4\, N^2 \pi r \left[\log_e\left(\frac{8r}{a}\right) - 2 \right] \tag{4}$$

where r is the radius of the detection coil and a is the radius of the (superconducting) wire. All units are SI (MKSA). Knowing the coil inductance L_{coil} and rewriting eq. 4 as

$$\Delta B = (L_{coil} + L_{SQUID})\Delta I/NA \tag{5}$$

we see that for a magnetometer, the maximum sensitivity will occur when the impedance of the detection coil matches that of the SQUID sensor ($L_{coil} = L_{SQUID}$). This can be seen by differentiating $\Delta B/\Delta I$ with respect to N. If increased sensitivity is needed, one should attempt to match impedances. Since the SQUID system has an output proportional to the input current, maximum sensitivity is obtained by using the input circuit that provides the maximum current into the SQUID and satisfies all other constraints of the experimental apparatus.

3.1. Detection Coils

Several factors affect the design of the detection coils **(3,4,6)**. These include the desired sensitivity of the system, the size and location of the magnetic field source and the need to match the inductance of the detection coil to that of the SQUID. The ability to separate field patterns caused by sources at different locations and strengths requires a good signal-to-noise ratio. At the same time, one has to find the coil configuration that gives the best spatial resolution. Unfortunately, these two tasks are not independent. For example, increasing the pickup-coil diameter improves field sensitivity, but sacrifices spatial resolution. In practice, system design is restricted by several constraints: the impedance and noise of the SQUID sensors, the size of the dewar, the number of channels, along with the distribution and strength of external noise sources.

Normally, SQUID magnetometers map the axial component of the magnetic field. It is also possible to monitor all three vector components of the magnetic field. This would require three times as many channels as a system that only measures axial fields. Since the volume currents (due to biological sources) are the main contributor to the non-axial field components, the additional information may be minimal. Figure 8 displays a variety of detection coils that have been used in making biomagnetic measurements. The magnetometer (fig. 8a) responds to the changes in the field penetrating the coil. More complicated coil configurations provide the advantage of discriminating against unwanted background fields from distant sources while retaining sensitivity to nearby sources

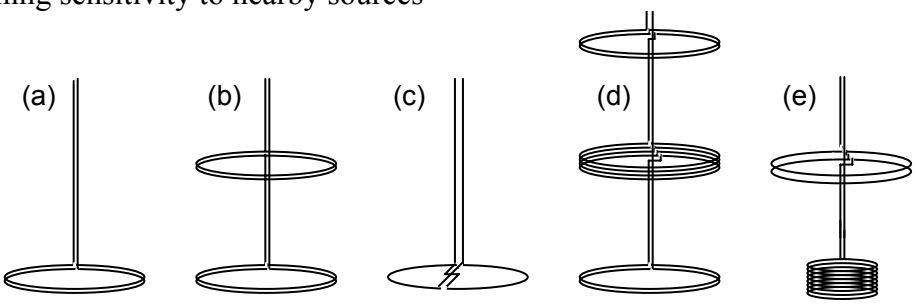

Fig. 8. a) magnetometer b) 1st derivative gradiometer c) planar gradiometer d) 2nd derivative gradiometer d) 1st derivative asymmetric gradiometer e) 2nd derivative asymmetric gradiometer; Courtesy of SJ Williamson

4.2. Gradiometers

Magnetometers are extremely sensitive to the outside environment. This may be acceptable if one is measuring ambient fields. If what is to be measured is close to the detection coil and weak, outside interference may prevent measurements at SQUID sensitivities. If the measurement is of a magnetic source close to the detection coil, a gradiometer coil may be preferred. The field of a magnetic dipole is inversely proportional to the cube of the distance between the dipole and the sensor. It follows that the field from a distant source is relatively uniform in direction and magnitude at the sensor. If we connect in series two identical and exactly parallel loops wound in opposite senses, separated by a distance b (the baseline), we obtain a coil (fig. 8b) that will reject uniform fields.

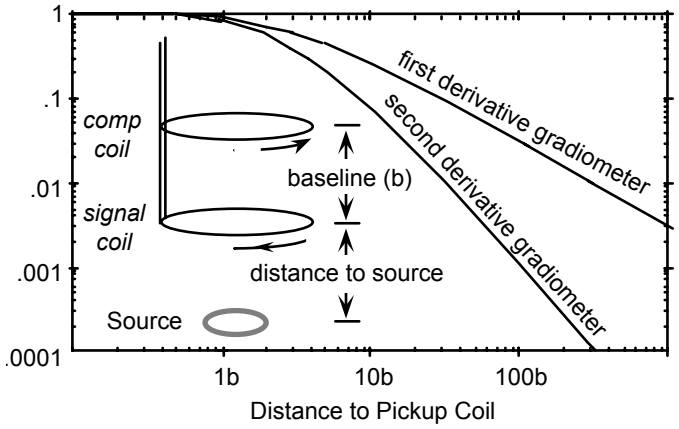

Fig. 9. Response of gradient coils relative to magnetometer response ($1/r^3$ suppressed)

Since the response of a single coil to a magnetic dipole goes as $1/r^3$, an object that is much closer to one coil than the other, will couple better to the closer coil than the more distant. Sources that are relatively distant will couple equally into both coils. For objects that are closer than 0.3b, the gradiometer acts as a pure magnetometer, while rejecting more than 99% of the influence of objects more than 300b distant (fig. 9). In essence, the gradiometer acts as a compensated magnetometer.
Unfortunately background fields are rarely uniform. However, if their sources are sufficiently remote, the gradient in the field over the sensing coils is both small and uniform. In this case, it is possible to use two gradiometers connected in series opposition to further minimize the response of the system to these sources (fig. 8d). This technique greatly reduces the sensitivity to environmental magnetic noise, both uniform fields and linear field gradients. This can increase the signal-to-noise ratio by about a factor of 10^6 above that achieved with a single loop magnetometer. The 2nd order configuration has enabled the recording of magnetic encephalograms in an unshielded urban environment **(1)**. This technique can obviously be extended to higher orders by connecting in series opposition two 2nd order gradiometers, etc.**(14)**. Doing so, however, reduces the sensitivity of the instrument to the signal of interest and may not significantly improve the signal-to-noise ratio.

Axial gradiometers, measuring the radial component of the field, have been popular because of the easy intuitive interpretation of the results. Another trend in multi-channel neuromagnetic instrumentation is the use of planar detection coils **(6)**. Planar coils are of interest because the construction would be simpler and interpretation of data is relatively simple (eq. 6). In practice, however, simple magnetometers are not feasible, even inside shielded rooms: mechanical vibrations of the dewar in the remnant magnetic field and nearby noise sources such as the heart may disturb the measurement. Because of the compact structure and excellent intrinsic balance of planar devices, thin-film gradiometers have definite advantages when designing systems requiring more than 100 channels. Analysis of the non-axial components of the magnetic field gradient may require additional data reduction techniques, but with the use of sophisticated computer modeling, not insoluble.

An asymmetric design (fig. 8e) has the advantage that the inductance (L_{signal}) of pickup coil(s) is much greater than the compensation coils (L_{comp}); therefore, greater sensitivity is achieved than with a symmetric design. The pickup coil should have smaller area but more turns than the other(s) so that its inductance is the dominant contribution to L_{coil}. A balanced gradiometer requires that $N_{signal}A_{signal} = N_{comp}A_{comp}$ where N is the number of turns and A the area of the pickup and compensation coils respectively. For a 1 cm diameter pickup coil ($N_{signal} = 4$) and a 2 cm compensation coil ($N_{comp} = 1$), 87% of the total inductance is associated with the pickup coil and higher sensitivity is achieved than with a symmetric coil. Another advantage is that the pickup coil diameter is reduced, leading to potentially higher spatial resolution. For an asymmetric gradiometer, maximum sensitivity will not occur when $L_{coil} = L_{SQUID}$. In this situation, the optimum condition for the number of turns N_{signal} in the signal coil is given by **(6)**

$$\left(L_{signal} + L_{comp} + L_{SQUID} + L_{leads}\right) - N_{signal}\frac{\partial}{\partial N_{signal}}\left(L_{signal} + L_{comp} + L_{leads}\right) = 0 \qquad (6)$$

Immunity to distant noise sources may depend critically on having a precise match (or balance as it is sometimes referred to) between the number of area-turns in the coils **(3,15)**. Should one coil have a larger effective diameter than the other, the response of the coil will not be that of a perfect gradiometer, but that of a gradiometer in series with a magnetometer. Typically, coil forms used to wind gradiometers can be machined (grooved) to achieve balances that range from 10,000 ppm (1%) to 1,000 ppm (0.1%). (Planar devices, through photolithography, can achieve lower levels — a factor of 10 or better.) Because a superconductor will expel flux (the Meissner effect), small superconducting trim tabs can be used to improve balance to the hundreds of ppm level. Improvements to the 1 - 0.1 ppm level can be achieved with adjustable trim tabs that are positioned when the magnetometer probe is at liquid helium temperatures. Reproducibility is limited to the 10 ppm level because of thermal cycling effects. If eddy current noise (due to the presence of normal metal conductors near the detection coils) is significant, system balance will show an 90° out-of-phase component that can not be balanced with superconducting trim tabs.
For multi-channel systems, it is not possible to use externally adjustable trim tabs (each tab tends to interfere with each other - the number of interactions goes as 3N factorial). The use of electronic balancing **(15,16)** can provide balance ratios at the ppm level. In this situation, three orthogonal magnetometers are used. Portions of the magnetometers' response are summed electronically with the gradiometers' input to balance out its effective magnetometer response. In addition to balancing with the three field components, it may be desirable to use a very short baseline gradiometer as a fourth "noise" channel for rejection of gradient noise. The major advantage of electronic balancing is significant improvement in immunity to low frequency environmental noise.

3.3. Multichannel considerations

Initially, biomagnetic measurements were carried out using single-channel magnetometers. Multiple placements were quite time consuming and could easily take as much as one week. Multi-channel systems allow the collection of data over multiple sites simultaneously. Such instruments not only make the measurements faster, but also give more reliable data. Ideally, a system should be able to cover the entire head and allow real-time measurements. Given a fixed SQUID sensitivity, the area to be covered and the desired spatial resolution will determine the number of channels in a multi-channel system. Unfortunately, magnetometer technology has not advanced to the stage where hundreds of channels in arbitrary configurations are readily available. A limited number of channels will require either a limited measurement region or that the magnetometer be sequentially moved to cover the desired area. The desire for real-time data acquisition has fueled the development of magnetometers with ever increasing numbers of channels. The first generation of multi-channel systems were primarily seven channels in a hexagonal array (fig. 10) **(16,17)**.

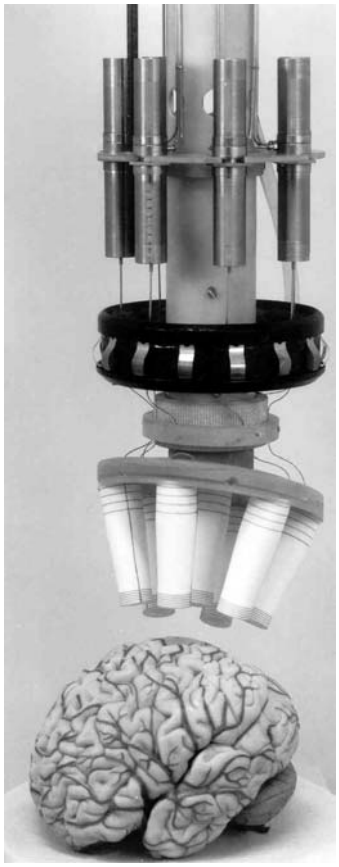

Fig. 10. Seven channel system with asymmetric first derivative coils **(ref. 17)**. Note coils are tilted at 30° to allow ease of placement near the side of the head. Courtesy of Olli Lounasmaa.

This was chosen to place the maximum number of channels in a nearly circular cross-section. The major constraint was to have the minimum diameter of the liquid helium dewar (see section on dewars) to keep the liquid helium consumption at a minimum. To gain additional head coverage, dual systems (fig. 1) can be used. The next generation of multi-channel systems adds an additional two (hexagonal) layers to give either 31 (Siemens KRENIKON™) or 37 (Biomagnetic Technologies model 700C Neuromagnetometer) channels. With coil-to-coil spacings of ~ 2 cm, these systems can cover a significant portion of the skull.

In determining the spacing between coils, the spatial frequency content of the signal to be measured must be determined. Field distributions caused by a current dipole in the brain have spatial frequencies between 10 and 30 m^{-1}, depending on the depth of the sources **(6)** corresponding to a suitable grid spacing of 20 ~ 30 mm. This implies the need for 100+ channels if the entire head is to be mapped without moving the magnetometer. If information on source localization is primarily contained in the region between the extrema (of the magnetic field patterns due to neurological activity), closer coil spacing will be needed. The argument is as follows: since localization depends on the ratio of signals in adjacent detection coils, the greatest information is found in the tangential derivative of the radial field ($\partial B_\rho/\partial\psi$). Computer simulations **(18)** indicate that for shallow dipole sources, it may be desirable to sample at 2 to 5 mm intervals. Similarly, multiple dipole sources can have higher field gradients than a single source, resulting in spatial frequencies significantly higher than 30 m^{-1}. Thus, if the entire head is to be covered, and the sources are both shallow and multiple, the number of channels required for real-time data acquisition could approach or even exceed 1000! In this (unlikely) situation, an all thin-film gradiometer would be the only practical device.

To determine where neural sources lie within the head it is necessary to measure accurately the position and orientation of each detection coil with respect to the head. Normally, the magnetometer is positioned with some alignment marks on the dewar and on the subject's head. Accurate positioning with this method can be difficult, especially if there is uncertainty in the position of the detection coils with respect to the dewar. The accurate location and orientation of the dewar with respect to the head can be determined by measuring the

magnetic field produced by current in small coils attached to the head **(6)**. Another technique **(19)** is to use three orthogonal coils in the receiver (attached to the dewar) and in the transmitter (on the head). From the measured mutual inductances, the position and the orientation of the magnetometer can be found. The accuracy of these two methods can be better than ±1 mm. Such methods also allow the shape of the head to be digitized for use in data analysis.

The magnetometer (and dewars) must be mounted on a sufficiently rigid platform that external vibrations will not cause movement of the detection coils. Because of the need to position the magnetometer, the system must be free to move in several different orientations. Ease of use requires at least five degrees of freedom. Independent movement should be provided along two orthogonal horizontal directions and the vertical direction, with rotation allowed about the vertical axis and the horizontal axis of the dewar. It may be desirable for the dewar to be rotated about its own axis if it is necessary that the individual sensors within the dewar be placed in a particular orientation.

4. DEWARS

The use of niobium SQUID sensors has required that the SQUID and detection coil(s) to operate well below their superconducting transition temperature of 9.3 K. The thermal environment for the SQUID sensor and detection coil has typically been liquid helium (at 4.2 K) contained in a special insulated vessel known as a dewar. Since the magnetometer must measure magnetic fields exterior to the dewar, the dewar must be magnetically transparent and metallic construction is not appropriate.

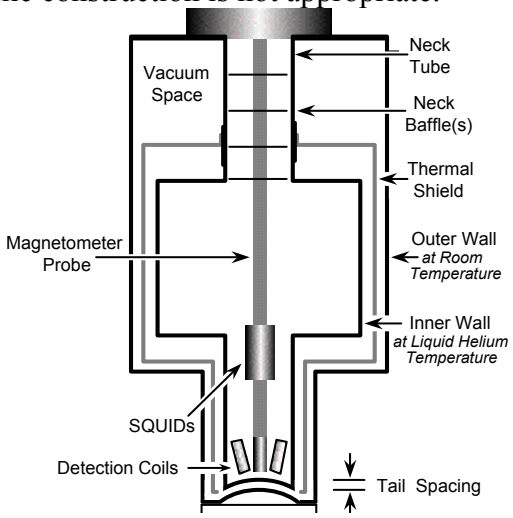

Fig. 11. Cutaway diagram of typical biomagnetic dewar

Figure 11 shows the typical design of a fiberglass dewar used for biomagnetic measurements **(20)**. The space between the inner and outer walls is evacuated to prevent thermal conduction between room temperature and the liquid helium chamber. Within the vacuum space, a thermal shield acts to reduce heat transfer by thermal (blackbody) radiation. A typical dewar uses a vapor-cooled radiation shield that is thermally anchored to the neck tube. A typical boil-off rate for a single channel magnetometer dewar (neck diameter = 5 cm) is ~ 1.3 liters of liquid helium/day. Multi-channel dewars, because of their larger neck tube may be more than double this. The "hold time", or time between liquid helium refills, for commercial dewars is typically a few days (twice/week) to slightly above one week. By increasing the belly diameter, it is possible to increase the hold time, but at a cost of increased weight and exterior dimensions. In an effort to get the detection coil(s) as close as possible to the object being measured, a "tailed" design is often used. This decreases the forces on the tail facing of the dewar and allows the use of thinner end pieces.

As the number of detection coils increases, the tail area increases, as do the forces on the tail. As the forces increase, the thickness of the tail piece must be increased to avoid structural collapse. Unless one can adjust the separation between the inner and outer tails when the dewar is cold, for a single channel magnetometer with a tail area of ~ 8 cm^2, the minimum tail spacing is ~ 9 mm. For a seven channel magnetometer (A ≈ 200

cm^2), the tail pieces are thicker and the minimum tail spacing is ~15 mm (fig. 1). The Siemens 31 channel KRENIKON system ($A \approx 400\ cm^2$) has a spacing of 25 mm. Placing the detection coils in the vacuum space between the inner and outer walls can reduce the effective tail spacing **(21)**. The use of Nb or NbTi ($T_c > 9$ K) can allow positioning the detection coil(s) closer to room temperature without loss of superconductivity. Placing the coils (or the entire SQUID and magnetometer in the case of a planar device) in vacuum may decrease tail spacing, but at a significant increase in complexity of construction.

The shape of the dewar tail is dependent on the application. Because the sensitivity of current neuromagnetic detection systems is limited, it is desirable for the detection coils to be as close to the skull as possible. If the primary region of interest is in the region of, say the temporal lobes, a flat-tail dewar may be preferred. The flat-tailed dewar allows the detection coils (on average) to be as close to the side of the head as possible (fig. 12). Other regions might require simple concave (spherical) tails with a radius to match the subject's head (figs. 10 and 13). The obvious problem is that there is a great variation in head shapes and sizes. As the number of channels/system grows, the need to have more complex, non-spherical dewar tails increases. When deciding on the dewar design desired, the user will need to take into account the specific application.

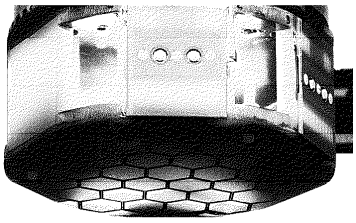

Fig. 12. Siemens KRENIKON™ detection coils.

Courtesy of Siemens AG, Erlangen, Germany.

Fig. 13. BTi model 700C Neuromagnetometer® detection coils.

Courtesy of Biomagnetic Technologies, Inc. San Diego, CA, USA.

Dewars for biomagnetic measurements are normally constructed of specially designed and selected materials to minimize their magnetic interactions with the SQUID sensors and detection coils. They are constructed of shatterproof fiberglass reinforced epoxy and are quite safe to use. Materials used are typically glass-fiber epoxy composites such as G-10 **(22)**. It may be of benefit to use a more costly material such as quartz cloth which has a lower magnetic susceptibility than G-10, especially in the vicinity of the detection coils. Because of the proximity to the detection coils, Johnson noise generated by eddy currents in the thermal shield can be significant. By using more resistive materials, eddy current noise can be reduced, but at the cost of increasing the susceptibility to rf interference (eq. 9). Avoiding connected conducting paths in the thermal shield can reduce this problem. With careful attention to dewar design, it has been possible to reduce this component of system noise to ~ 5 fT/√Hz.

4.1. Closed Cycle Refrigeration

As an alternative to the use of liquid helium, closed cycle refrigeration would be desirable for several reasons. These would include reduction of operating costs, use in remote locations, avoiding interruptions in liquid helium deliveries, safety; and the convenience of not having to transfer helium every few days. One such system incorporates a Gifford-McMahon (GM) closed cycle refrigerator and a Joule-Thomson (JT) cooling circuit **(19)**. It provides cooling of a dc SQUID and a single second-order gradiometer detection coil with noise levels below 20 fT/√Hz. The use of a JT cycle for the low temperature stage eliminates the noise problems associated with the temperature fluctuations of an all mechanical design and provides the 5 K environment required for low-noise SQUID operation. This system has the unique ability to operate in an inverted position. Such a system can be used to monitor activity at the side of the upright head, or activity low on the posterior region of the head. Scaling such a system up to service a large multi-channel array of

SQUID sensors could have significant impact on the acceptance of SQUID magnetometers in clinical environments.

5. Environmental Noise

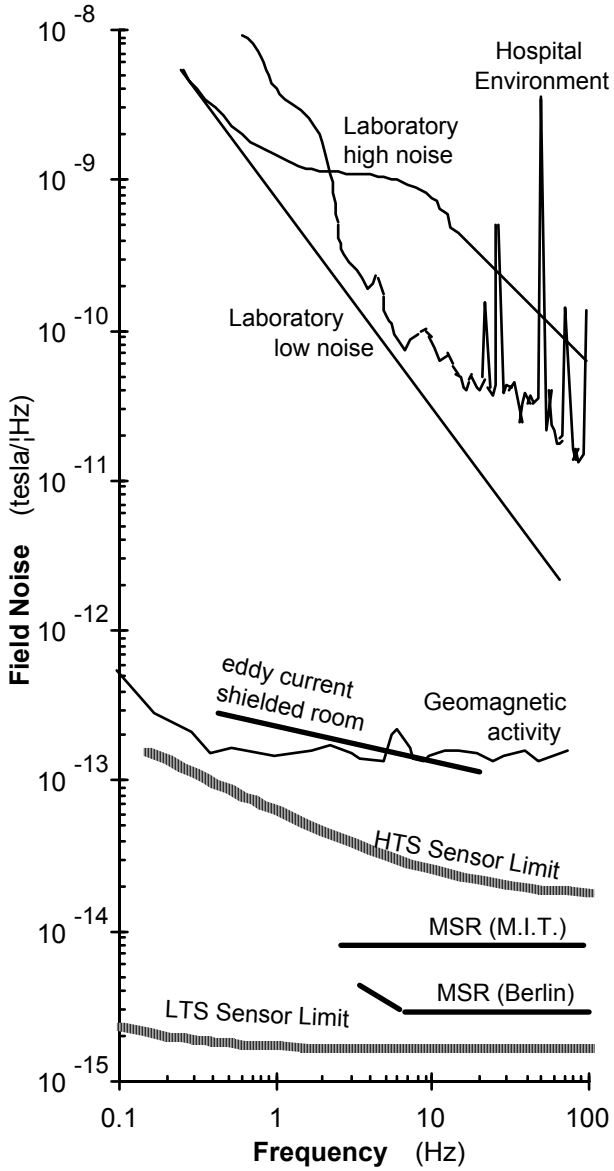

Fig. 14. rms field noise spectra in various environments as a function of frequency. Courtesy of SJ Williamson

The greatest obstacle to the widespread use of SQUID magnetometers is environmental noise (fig. 14). The SQUID magnetometer must operate in an environment - the magnetic field of the earth — that can be 10 orders of magnitude greater than its sensitivity. The magnetic field at the surface of the earth is generated by a number of sources **(23)**. There exists a background field of ≈ 50 microtesla (½ gauss) with a daily variation of ± 0.1 microtesla. In addition there is a contribution (below 1 Hz) from the interaction of the solar wind with the magnetosphere. The amplitude of this ac field is frequency dependent, generally decreasing as the frequency increases. The remaining contributions to external magnetic fields are primarily man-made. These can be caused by the following: structural steel and other localized magnetic materials such as furniture and instruments that distort the earth's field and result in field gradients; moving vehicles that generate transient fields; electric motors; elevators; radio, television, and microwave transmitters; and the ever present powerline electromagnetic field and its harmonics.

6. Noise Reduction

One method to attenuate external noise sources is with an eddy current shield. Time varying electromagnetic fields induce circulating currents in conducting materials. These eddy currents generate fields that act to cancel the externally applied fields within the conducting material. Eddy current shields make this use of Lenz's law to attenuate external fields inside a conducting enclosure. The shielding effect is determined by skin depth, λ — the distance at which the electromagnetic wave is attenuated by a factor of 1/e. For a sinusoidal varying wave, the skin depth can be expressed as

$$\lambda = \sqrt{\rho / \pi \mu_o f} \tag{7}$$

where f is the frequency of the applied field, ρ the electrical resistivity and μ_o the magnetic permeability of free space. As an example, the skin depth of copper at 4.2 K is ~ 2 cm at 100 Hz. In situations where the wall thickness is much less than λ, external fields are attenuated according to the formula

$$\frac{H_{internal}}{H_{external}} = \frac{1}{1 + (2\pi f L / R)^2} \tag{8}$$

where L is the inductance of the enclosure and R is the resistance along the path of current flow. Unfortunately, induced currents in the shield generate magnetic field noise. For a cylindrical shape, this noise is equivalent to

$$B_{rms} / \sqrt{Hz} = \sqrt{\frac{64 \pi k_B T t}{h d \rho \times 10^{-21}}} \tag{9}$$

where h, d, and t are the length, diameter and thickness of the can. Because of noise considerations, eddy current shields that are to be placed near the detection coils should be made from relatively poor conductors such as BeCu ($\rho \approx 8 \times 10^{-8}$ Ω-m at 4.2 K). The cut-off frequency is given by $f_{-3dB} \approx \rho / 4\pi dt \times 10^7$ (Hz). Another approach is to use eddy current shielding to shield the entire measuring system.

6.1. Shielded Rooms

As seen in fig. 14, hospitals can be extremely noisy due to electromagnetic radiation, low-frequency magnetic noise, and noise at intermediate frequencies contributed by machinery and power lines. Use of second or higher-order gradiometers can overcome much of this noise in a normal laboratory setting; but greater noise reduction may be needed for routine clinical applications. Environmental noise can be particularly severe at low frequencies. A site survey prior to system installation (or purchase) can determine the ambient noise and the level of shielding required. An extremely sensitive flux-gate magnetometer or preferably, a SQUID magnetometer should be used for the site survey (including inspection of alternate sites).

Magnetic and eddy current shielding can greatly reduce the influence of external electromagnetic fields **(24)**. Using the resistivity of conducting materials such as copper or aluminum ($\rho \approx 2 \times 10^{-8}$ Ω·m at room temperature), we see that the skin depth is less than 0.1 mm at MHz frequencies, but increases to more than 2 cm at 10 Hz. Thus fields with high frequencies can easily be attenuated (eq. 8) by using very thin metal plates, whereas low frequencies (*e.g.*, 50 or 60 Hz power line frequencies) require walls with thickness exceeding several centimeters. One such eddy current room has been constructed **(25)** from high purity aluminum. Using 1.88 cm thick walls, its dimensions were 3.6 meters by 2.44 meters and 2.5 meters in height. Shielding was more than 40 dB at 60 Hz with improved performance at higher frequencies. The equivalent field noise was less than 200 fT/√Hz at frequencies above 1 Hz.

The need for shielding at lower frequencies has led to the use of magnetically shielded rooms (MSR). In the situation where the wall thickness of the enclosure "t" is much greater than the skin depth, the attenuation goes as $(r/\lambda)e^{t/\lambda}$. If pure eddy current shielding is used, this would require wall thickness' that could exceed one meter or more (below 1 Hz). For a ferromagnetic material, the permeability of the material [$\mu = \mu_o(1 + \chi)$] replaces μ_o in eq. 8. The shielding is due to the fact that flux prefers the path with the highest

permeability. Since magnetically "soft" materials (*e.g.*, mu-metal®) can have permeabilities that exceed 10^4, the external magnetic flux is routed around the walls, avoiding the interior. The use of multiple shields can act to further shield the interior of a MSR. For the MSR at Berlin (fig. 14) shielding factors exceeded 10^4 at frequencies above 0.01 Hz. Noise levels within a MSR can be below 3 fT/√Hz (sufficiently low that the room noise is below that of the SQUID magnetometer).

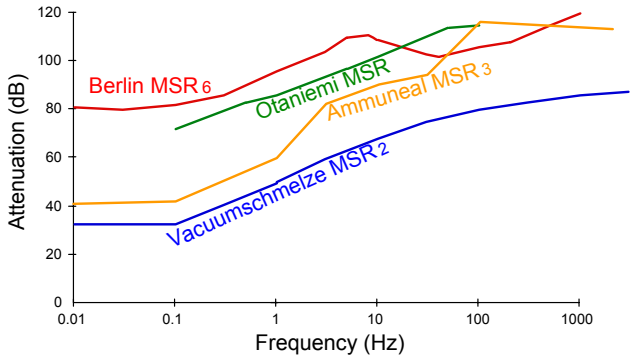

Fig. 15. Commercial magnetically shielded room showing first layer of mu-metal shielding and rigid aluminum frame. Courtesy of Vacuumschmelze GmbH, Hanau, Germany.

Fig. 16. Shielding factors at various frequencies of three MSRs. Berlin MSR — ref. 24, Otaniemi MSR — ref. 6, Vacuumschmelze MSR —fig. 15.

A major drawback of a MSR is its cost. By reducing the number of mu-metal shields, cost can be reduced, but at the expense of a decreased shielding factor. If the detection coils(s) are in a magnetometer configuration, this may not be a wise idea. However, the use of even first derivative gradiometer coils can permit a reduction in the needed shielding factor. Commercially available MSR's offer such a compromise, using two layers of mu-metal with a aluminum eddy current shield for additional attenuation of high frequencies. A typical commercial room consists of an mu-metal inner shield mounted on 8-mm thick aluminum plate that acts as an eddy-current magnetic and radio-frequency shield. This inner shell is supported by a 15 cm aluminum framework (fig. 15). The outer surface of the framework is covered by a second mu-metal shield. The ceiling of the MSR has support railings that can be used to suspend gantries for holding the dewar containing the magnetometers. Figure 16 shows the attenuation for a such a MSR **(19)**. The shielding is not as effective as for MSRs having three separated layers of magnetic shielding **(6,24)**, but offers significantly lower cost and greater interior space.

6.3 Data Acquisition

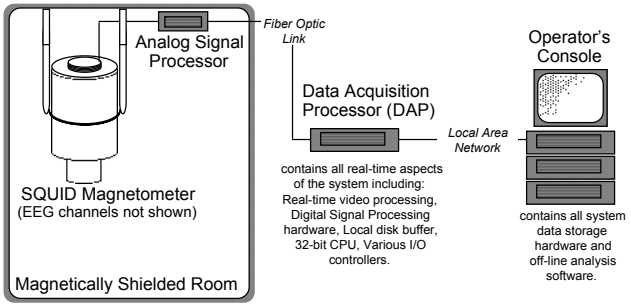

Fig. 17. Typical acquisition hardware consisting of an analog signal processor, a dedicated real-time data acquisition processor and an operator's console.

The first link in the data acquisition chain is a low-level signal processor. It might reside inside the magnetically shielded room, in close proximity to the SQUIDs. Microprocessors used in data acquisition systems operate at tens of MHz and even the best rfi shielding is insufficient to prevent overload when a computer is operated inside a shielded room. The low-level processor would amplify and filter the multichannel (typically analog) SQUID data (and EEG information if available), digitizing the resulting high-level, conditioned signal. It should be able to digitize multiple signal channels (as well as any reference

channels used for electronic balancing). Ideally, one to three (analog) signal processors would be connected to the system, one dedicated to the multichannel sensors (two, if a dual dewar system is used) and one dedicated to electrical signals (assuming simultaneous EEG measurements).

A typical data acquisition processor (DAP) — located outside the MSR — might consist of a 32-bit processor, digital signal processor hardware and various disk and I/O controllers. Ideally, it should control various high-speed and real-time aspects of the system, including stimulus control, data acquisition I/O (commands out, data in) and high-speed post-acquisition processing. A desirable feature is a video controller board for real-time waveform data and general system status displays along with an analog output board for output to oscilloscope (such as the console CRT). The video controller should be capable of displaying multiple channels of incoming analog data in real-time.

Data storage requirements for MEG can be quite severe. Epoch durations for evoked response modes range from a minimum of 15 milliseconds to a maximum of 20 seconds or more in the evoked response modes. Some data analysis paradigms require very short epochs (15 milliseconds) at high repetition rates (11 per second) for many repetitions (1,500 or more). Situations can arise where continuous data must be recorded for at least one hour at sampling rates in the 100 to 400 Hz range. The DAP should have enough RAM memory and disk buffer space to allow storage of high volumes of data from the analog signal processor without overwriting the existing data. It is preferable to have at least 300 megabytes of disk storage and at least 4 megabytes of RAM memory local to the DAP itself. The DAP disk should be able to store at least 1 megabyte of data per second. The DAP must provide enough flexibility to support both continuous data and multi-epoch (evoked response) types of recording paradigms.

MEG Software is a critical part of any system. Ideally, the software should be programmed in a real-time executive environment. This provides high-speed system response to interrupt requests from the various I/O controllers. The digital signal processing portion of the DAP can be programmed via machine code to achieve the fast processing times necessary for its applications. These applications include noise-reduction, cross-correlation, decimation and other real-time algorithms. Data analysis packages are in their infancy. At a minimum, the system should be able to calculate equivalent dipole strengths and locations, preferably on a three-dimensional grid. The combination of hardware and software should be adequate for the proposed work. If not, significant amounts of effort will be expended to get the information into a usable form.

7. High Temperature Superconductivity

The discovery of high temperature superconductivity has led to the possibility of SQUID magnetometers operating at temperatures well above the boiling point of liquid nitrogen **(26)**. If feasible, high temperature superconductivity (high-T_c) could have significant impact on the cryogenic requirements of SQUID magnetometers. Magnetometer noise levels below 10 fT/√Hz require SQUID sensors with E_N's below 10^{-31} J/Hz (eqs. 1,3). Since SQUID noise scales with temperature (eq. 2), any SQUID operating at 77 K would have noise levels ~20 times higher than a SQUID operating at 4 K. Thus the use of a high-T_c SQUID (fig. 6) for neuromagnetic measurements is unlikely. If truly superconducting, wire or films could be used to make detection coils that would operate quite close to T_c (> 90 K). High-T_c materials may make it possible to get the sensors closer to the head, resulting in increased signal strength **(21)**. At the present time, poor flux pinning in the known high-T_c materials gives rise to a phenomenon known as flux creep **(27)**. This is manifested as an effective resistance and might reduce the sensitivity of high-T_c detection coils at low frequencies. Should improved materials rectify this situation, a good combination of high sensitivity and close-to-the-head sensors might be obtained with a hybrid structure, with a high T_c pickup coil and a SQUID at 4.2K.

8. System Performance

System performance is usually given in terms of magnetic field noise in a 1 Hz bandwidth. Single channel second derivative gradiometers using rf commercial SQUIDs typically had $B_N \approx 35$ fT/√Hz. dc SQUID versions were typically 20 fT/√Hz. The first multi-channel systems were also at the 20 fT/√Hz level. The availability of high performance thin film SQUIDs **(17)** has led to the construction (fig. 10) of a 7-channel system with an ultimate field sensitivity of ~ 1 fT/√Hz. Dewar noise (section 4) limits system performance to ~ 5 fT/√Hz.

The choice of detection coil design is very much dependent on what is to be measured. Although many systems are described in terms of their ability to detect magnetic dipoles - a valid assumption when considering noise sources - the magnetic dipole does not provide a good model of neurological sources. The most common source model in electrophysiology is that of the current dipole. The strength *Q* of a current dipole has the dimension of current times length and the unit of ampere-meter. It is represented by a vector whose direction coincides with the direction of the current. The current dipole is a simplified representation for much more complex patterns of current which exist at the cellular level **(1)**. The current dipole is useful in that more elaborate extended sources can be represented by an array of individual current dipoles. The response of a simple magnetometer to a current dipole in free space can be expressed by **(28)**

$$Q_{MIN} = \frac{\text{š}\ \Phi_{MIN}\sqrt{m}}{\mu_o \sqrt{\frac{r}{\rho}}\left[\left(1-\frac{m}{2}\right)K(m) - E(m)\right]} \tag{10}$$

$$m = \frac{4\,r\,\rho}{\sqrt{(r+\rho)^2 + z^2}} \tag{11}$$

where Q_{MIN} is the smallest current dipole that can be detected, Φ_{MIN} is the minimum detectable magnetic flux in the pickup coil (see eq. 3), μ_o (permittivity of free space) = $4\pi \times 10^{-7}$ henries/meter, r is the radius of the pick-up coil, ρ is the off-axis distance (in cylindrical coordinates), z is the axial distance of the current dipole (*Q*) below the bottom of the pick-up coil and K and E are elliptical integrals of the first and second kind. For a gradiometer, one must sum the response of all the coil windings and take into account the baseline of the gradiometer. The tail spacing of the dewar must not be neglected when determining z.
For a first derivative gradiometer where B_{MIN} = 5 fT/√Hz, r = 1 cm and six turns in the pickup coil **(17)**, we find that $\Phi_{MIN} = 9.4 \times 10^{-18}$ Webers. These values can be inserted into eq. 6 to determine Q_{MIN} vs. position (fig. 18). As can be seen, coil sensitivity for a current dipole goes as $1/r^2$, rather than the $1/r^3$ expected for a magnetic dipole.

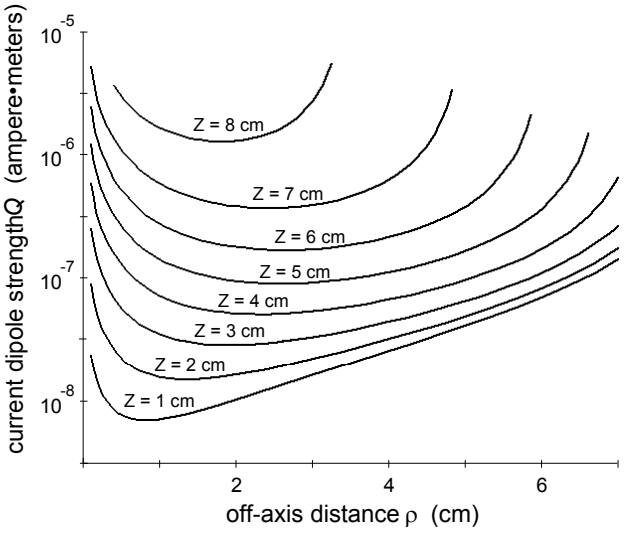

Fig. 18. Minimum detectable current dipole as a function of off-axis position (ρ) and depth (z)

9. Summary

In considering what type of MEG system is needed, there are four main considerations.

1) Ambient Magnetic Noise at the Intend Site(s): The need to reject external noise will determine the need for a shielded room. Here manufacturer's claims can be compared in terms of magnetic field sensitivities ($B_N/\sqrt{Hz}$) at the measurement site. There are several tradeoffs to consider. A relatively quiet environment may allow use of a less expensive eddy current shielded room combined with second derivative gradiometer coils. A harsher environment might need a MSR, but gain in sensitivity by using first derivative gradient coils. A truly hostile environment could require multiple eddy current shields combined with a MSR using three or more layers of mu-metal.
2) Head Coverage and Spatial Resolution: The number of channels will roughly determine the number of times the dewar(s) must be moved to cover the entire region of interest. Until MEG systems are available that can cover the entire head, coverage will be an important factor. Spatial resolutions (related to the diameter of the pickup coils and their spacing should be adequate for all intended measurements.
3) Required Sensitivity: Since object to be studied are current dipoles, magnetic field sensitivities (in $fT/\sqrt{Hz}$.) are not appropriate. This should be in terms of sensitivity to a current dipole measured in ampere·meters (eq. 10) as a function of depth below the bottom of the dewar tail.
4) Data acquisition systems and system software: Major considerations include:
   at what rate is data to be gathered?

   the total amount of data to be gathered in a single session?

   must the data be processed real time?

   how is the data to be interpreted?

   how is the data to be displayed?

By examining the above factors, it should be possible to compare available systems for neuromagnetic measurements and determine which system is appropriate for your needs.

Acknowledgments

The author would like to thank Stephen Robinson and Claudia Tesche for a number of helpful conversations and comments.

REFERENCES

1 Williamson SJ, Kaufman L. Biomagnetism. J. Magn. Mag. Mat. 1981; 22: 129-202

2 Giffard RP, Webb RA, and Wheatley JC. Principles and Methods of Low-Frequency Electric and Magnetic Measurements Using an rf-Biased Point-Contact Superconducting Device. J. Low Temp. Phys. 1972; 6: 533-610

3 Sarwinski RE. Superconducting instrumentation. Cryogenics, 1977; 17: 671-679

4 Romani G-L, Williamson SJ, Kaufman L. Biomagnetic instrumentation. Rev. Sci. Instrum. 1982; 53: 1815-1845

5 Fagaly RL. Superconducting magnetometers and instrumentation. Sci. Prog., Oxford 1987; 71: 181-201

6 Ilmoniemi R, Knuutila J, Ryänen T and Seppä H. Multi-SQUID devices and their applications. In: Brewer DF, ed. Progress in Low Temperature Physics, vol XII. Amsterdam:Elsevier, 1989; 1-63

7 Clarke J. Ultrasensitive measuring devices. Physica 1984; 126B: 441-448

8 Van Duzer T., Turner CW. Principles of Superconductive Devices and Circuits, New York: Elsevier, 1981

9 Josephson BD. Possible new effect in superconductive tunneling. Phys. Lett. 1962; 1: 251-253

10 Tesche CD, Clarke J. DC SQUID: noise and optimization. J. Low Temp. Phys. 1982; 29: 301-331

11 Awschalom DD, Rozen JR, Ketchen MB, et al. Low-noise microsusceptometer using nearly quantum limited dc SQUIDs. Appl. Phys. Lett. 1988; 53: 2108-2010

12 Simmonds MB, Giffard RP. Apparatus for reducing low frequency noise in dc biased SQUIDs. United States Patent No. 4,389,612. 1983

13 Grover FW. Inductance Calculations, Working Formulas and Tables, New York: Dover, 1962

14 Vrba J, Fife AA, Burbank MB, H. Weinberg H, Brickettt PA. Spatial discrimination in SQUID gradiometers and 3rd order gradiometer performance. Can. J. Phys. 1982; 60: 1060-1073

15 Jaworski FB, Crum DB. Sources of Gradiometer Imbalance and Useful Balancing Techniques. In:Weinstock H, Overton WC, eds. SQUID Applications to Geophysics, Tulsa, OK:Society of Exploration Geophysicists, 1981; 19-25

16 Crum DB, Hirschkoff EC, Marsden R, Smilo S. Design and performance of a 14-channel neuromagnetometer system. IEEE Transactions on Biomedical Engineering 1985a; BME-32: 890-895

17 Knuutila J, Ahlfors S, Ahohen A, et al. Large-area low-noise seven-channel dc SQUID magnetometer for brain research. Rev. Sci. Instrum. 1987; 58: 2145-2156

18 SE Robinson, private communication

19 Buchanan DS, Paulson DN, Williamson SJ. Instrumentation for clinical applications of neuromagnetism. In:Fast RW, ed. Advances in Cryogenic Engineering, vol 33. New York: Plenum, 1988; 97-106.

20 Crum DB. The design and use of dewars for biomagnetic measurements. In:Weinberg H, Stroink G, Katila T, eds. Biomagnetism: Applications & Theory, Proceedings of the Fifth International Conference on Biomagnetism , New York: Pergamon Press, 1985b; 21-28

21 Wikswo JP. High-resolution measurements of biomagnetic fields. In:Fast RW, ed. Advances in Cryogenic Engineering, vol 33. New York: Plenum, 1988; 107-116

22 Kelly B. Building in Fiberglass. Yacht Racing/Cruising 1982; July/August

23 Vozoff K. The Magnetotelluric Method in the Exploration of Sedimentary Basins. Geophysics 1972; 37: 98-114

24 Mager A. The Berlin magnetically shielded room (BMSR), Section A: Design and Construction. In:Erné SN, Hahlbohm H-D, Lübbig H, eds. Biomagnetism, Berlin: Walter de Gruyter, 1981; 51-78, see also pages 79-87, 89-94

25 Stroink G, Blackford B , Brown B, Horacek M. Aluminum shielded room for biomagnetic measurements. Rev. Sci. Instrum. 1981; 52: 463-468

26 Clarke J, Koch RH. The Impact of High-Temperature Superconductivity on SQUID Magnetometers. Science 1988; 242: 217-223

27 Yeshurun Y, Malozemoff AP. Giant Flux Creep and Irreversibility in an Y-Ba-Cu-O Crystal: An Alternative to the Superconducting-Glass Model. Phys. Rev. Lett. 1988; 60: 2202-2205

28 Wikswo JP. Optimization of SQUID differential magnetometers. In: Deaver BS, Falco CM, Harris JH, Wolf SA eds. Future Trends in Superconductive Electronics, AIP Conf. Proc vol 44. New York: Am. Inst. Phys, 1978; 145-149